

# Volcanic forcing improves Atmosphere-Ocean Coupled General Circulation Model scaling performance

D. Vyushin,<sup>1</sup> I. Zhidkov,<sup>1</sup> S. Havlin,<sup>1</sup> A. Bunde,<sup>2</sup> and S. Brenner<sup>2</sup>

Received 15 January 2004; revised 3 March 2004; accepted 28 April 2004; published 28 May 2004.

[1] Recent Atmosphere-Ocean Coupled General Circulation Model (AOGCM) simulations of the twentieth century climate, which account for anthropogenic and natural forcings, make it possible to study the origin of long-term temperature correlations found in the observed records. We study ensemble experiments performed with the NCAR PCM for 10 different historical forced simulations, including *no forcings*, *greenhouse gas*, *sulfate aerosol*, *ozone*, *solar*, *volcanic forcing* and various combinations, such as *natural*, *anthropogenic* and *all forcings*. We compare the scaling exponents characterizing the long-term correlations of the observed and simulated model data for 16 representative land stations and 16 sites in the Atlantic Ocean for these forcings. We find that inclusion of volcanic forcing in the AOGCM considerably improves the PCM scaling behavior. The simulations containing volcanic forcing are able to reproduce quite well the observed scaling exponents for the land with exponents around 0.65 independent of the station distance from the ocean. For the Atlantic Ocean, simulations with the volcanic forcing slightly underestimate the observed persistence exhibiting an average exponent 0.74 as compared to 0.85 for the Kaplan reconstructed data. *INDEX TERMS*: 0370 Atmospheric Composition and Structure: Volcanic effects (8409); 0910 Exploration Geophysics: Data processing; 3309 Meteorology and Atmospheric Dynamics: Climatology (1620); 4532 Oceanography: Physical: General circulation; 7538 Solar Physics, Astrophysics, and Astronomy: Solar irradiance. **Citation**: Vyushin, D., I. Zhidkov, S. Havlin, A. Bunde, and S. Brenner (2004), Volcanic forcing improves Atmosphere-Ocean Coupled General Circulation Model scaling performance, *Geophys. Res. Lett.*, 31, L10206, doi:10.1029/2004GL019499.

## 1. Introduction

[2] While many modelers and climatologists focus their studies on trends caused by natural and anthropogenic forcings during the twentieth century [e.g., *von Storch and Floeser*, 1999; *Mitchell et al.*, 2001; *Meehl et al.*, 2003; *Ammann et al.*, 2003], we here focus on another important aspect of temperature anomalies - long-term correlations. One of the first studies on the question how general circulation models reproduce observed climate variability was performed by [*Manabe and Stouffer*, 1996]. Using

power spectrum analysis, which is affected by nonstationarities in time series, they argue that the GFDL AOGCM reproduced the natural climate variability on decadal and centennial scales correctly for a 1000 year control run integration. Several recent studies of [*Koscielny-Bunde et al.*, 1996, 1998; *Pelletier and Turcotte*, 1997; *Talkner and Weber*, 2000; *Pelletier*, 2002; *Caballero et al.*, 2002; *Eichner et al.*, 2003] clearly demonstrate that surface air temperature (SAT) anomalies are long-term correlated with a fluctuation exponent  $\alpha$  close to 0.65. On the other hand, results of [*Bell et al.*, 2000; *Govindan et al.*, 2001, 2002; *Syroka and Toumi*, 2001; *Vjushin et al.*, 2002] indicate that AOGCMs underestimate surface air temperature (SAT) persistence for control run, greenhouse gas forcing only and greenhouse gas forcing plus sulfate aerosols forced simulations. In contrast, recent studies of HadCRUT2 data [*Fraedrich and Blender*, 2003] and NCEP reanalysis data [*Blender and Fraedrich*, 2003] claim that inner continental regions do not show long-term correlations, and thus AOGCMs successfully reproduce the natural persistence for the control run and greenhouse gas forcing only forced simulations. Recently, this claim was tested on observed records by [*Bunde et al.*, 2004] with the finding that the SAT fluctuation exponents for continental sites do show long-term correlation and the  $\alpha$  values do not depend on the distance of the site from the ocean.

[3] In this Letter we show that the recent Parallel Climate Model (PCM) simulations properly reproduce the observed long-term correlations for SAT on land only for those runs that include volcanic forcing. These runs also show better scaling performance over the ocean than the other runs.

## 2. Observed and Simulated Data

[4] In order to present the land-surface temperature profile for the last century, 16 observed daily maximum temperature time series are considered. They have been collected from different representative weather stations around the globe for the following sites: Vancouver, Tucson, Cheyenne, Luling, Brookings, Albany, Oxford, Prague, Kasan, Tashkent, Surgut, Chita, Seoul, Jakutsk, Melbourne and Sydney. We also analyze the gridded monthly mean sea surface temperature (SST) for 16 sites in the Atlantic ocean with a spatial resolution of  $2.5^\circ \times 2.5^\circ$  for the period of 1900–2002 from the Kaplan Extended SSTA data set [see also *Monetti et al.*, 2003]. For 1900–1981 this is the analysis of [*Kaplan et al.*, 1998] which uses optimal estimation in the space of 80 empirical orthogonal functions (EOFs) in order to interpolate ship observations [*Parker et al.*, 1994]. The data after 1981 consists of gridded data from the National Center for Environmental Prediction optimal interpolation analysis, which combines ship observations with remotely sensed data [*Reynolds and Smith*, 1994].

<sup>1</sup>Minerva Center and Department of Physics, Bar-Ilan University, Ramat-Gan, Israel.

<sup>2</sup>Institut für Theoretische Physik III, Justus-Liebig-Universität Giessen, Giessen, Germany.

<sup>3</sup>Department of Geography, Bar-Ilan University, Ramat-Gan, Israel.

[5] The model considered in our study is the Parallel Climate Model, which was developed at the National Center for Atmospheric Research (NCAR). It is a fully coupled global ocean-atmosphere-sea ice-land surface model that produces a stable climate without flux adjustment. The horizontal resolution of the atmosphere is equivalent to  $2.8^\circ \times 2.8^\circ$ , with 18 levels in the vertical. Resolution of the ocean is roughly  $2/3^\circ$ , increasing to  $1/2^\circ$  at the equator, with 32 levels. The detailed description of the model and results from experiments using various forcings and their combinations may be found in [Washington *et al.*, 2000], [Dai *et al.*, 2001], [Meehl *et al.*, 2003], and [Ammann *et al.*, 2003].

[6] Here we study 10 forcing combinations as indicated in the caption of Figure 3. Greenhouse gas forcing is based on historical records of  $\text{CO}_2$ ,  $\text{N}_2\text{O}$ ,  $\text{CH}_4$ , CFC-11, CFC-12, and ozone [Dai *et al.*, 2001]. Evolution of direct forcing from tropospheric sulfate aerosol is reported by [Kiehl *et al.*, 2000]. Historical changes of solar irradiance were reconstructed by [Hoyt and Schatten, 1993] and volcanic forcing by [Ammann *et al.*, 2003]. The period of all experiments is 1890–1999.

[7] For the no forcings and solar+volcanic forced simulations we analyze the available 3-member ensembles, whereas for other simulations 4-member ensembles are available. For each simulation, we selected the temperature records of the 4 grid points closest to each site, and bilinearly interpolated the data to the location of the observed site.

### 3. Methodology

[8] For each record, we analyse daily (or monthly) temperature anomalies  $\Delta T_i$ . The  $\Delta T_i$  are called long-term correlated if their autocorrelation function  $C(s)$  decays with time lag  $s$  by a power law

$$C(s) \sim s^{-\gamma}, \quad 0 < \gamma < 1. \quad (1)$$

To overcome possible nonstationarities in the data, we do not calculate  $C(s)$  directly. Instead we construct the cumulated temperature anomalies  $Y_n = \sum_{i=1}^n \Delta T_i$  (“the profile”,  $n$  is a month index, it varies from 1 to a time series length) and study the fluctuation function  $F(s)$  of the profile in segments of length  $s$  by using the second order detrended fluctuation analysis (DFA2) [Peng *et al.*, 1994; Kantelhardt *et al.*, 2001]. In DFA2 we determine in each segment the best second-order polynomial fit of the profile. The standard deviation of the profile from these polynomials represents the square of the fluctuations in each segment. By DFA2, we eliminate possible nonstationarities in observed records due to changing instrumentation, location, or local environment [Kantelhardt *et al.*, 2001].

[9] The fluctuation function  $F(s)$  is the root mean square of the fluctuations in all segments. For the relevant case of long-term power-law correlations given by Equation (1), with  $0 < \gamma < 1$ , the fluctuation function  $F(s)$  increases according to a power law,

$$F(s) \sim s^\alpha, \quad \alpha = 1 - \frac{\gamma}{2}. \quad (2)$$

For uncorrelated data (as well as for short-range correlations represented by  $\gamma \geq 1$  or exponentially decaying correlation

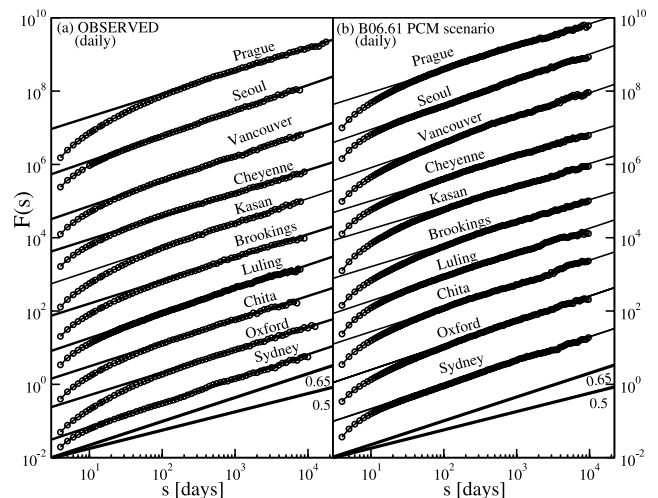


**Figure 1.** DFA2 fluctuation functions  $F(s)$  for the daily surface air maximum temperature anomalies at 10 land sites: (a) observed data and (b) NCAR PCM B06.61 (all forcings) simulated data. The scale of  $F(s)$  is arbitrary. The straight lines crossing each curve represent the best asymptotic fit. The two lines shown at the bottom have slopes 0.65 and 0.5.

functions), we have  $\alpha = \frac{1}{2}$ . For long-term correlations we have  $\alpha > \frac{1}{2}$ .

### 4. Results and Discussions

[10] First we plot the results of DFA2 (DFA curves of higher order show the same performance) for the observed daily maximum temperature (Figure 1a) and NCAR PCM simulations from the B06.61 run (Figure 1b). Run B06.61 represents one of the runs from the all forcings ensemble. All curves are shown in a double logarithmic presentation. We plot 10 typical DFA curves chosen from our 16 sites over land. The sites chosen include coastal, near coastal, and inland locations.

[11] The approximate period of the observed records is 1880–1990, with the maximum length for Prague (1775–1992) and the minimum for Seoul (1908–1993). The period of the B06.61 run is 1890–1999. The slopes in Figure 1a correspond to fluctuation exponents of the observed SAT anomalies, and vary from 0.62 to 0.68, with an average close to 0.65. Figure 1a demonstrates that SAT anomalies for all sites studied obey long-term power-law correlations independent of the distance from the nearest ocean. The slopes in Figure 1b range from 0.62 to 0.69. Comparing Figures 1a and 1b shows that the scaling of the NCAR PCM output agrees quite well with the scaling of the observed data over land.

[12] Figure 2 shows DFA2 curves for the 10 sites in the Atlantic ocean for the Kaplan reconstructed monthly SST anomalies (Figure 2a) and for the NCAR PCM monthly averaged SST anomalies from the all forcings B06.61 run (Figure 2b). The slopes for the reconstructed SSTA vary from 0.71 in the equatorial part of the Atlantic to 1.0 in the Northern Atlantic, with an average of 0.85. The SSTA exponents characterizing the memory effect on decadal and centennial scales seem to depend on complex ocean

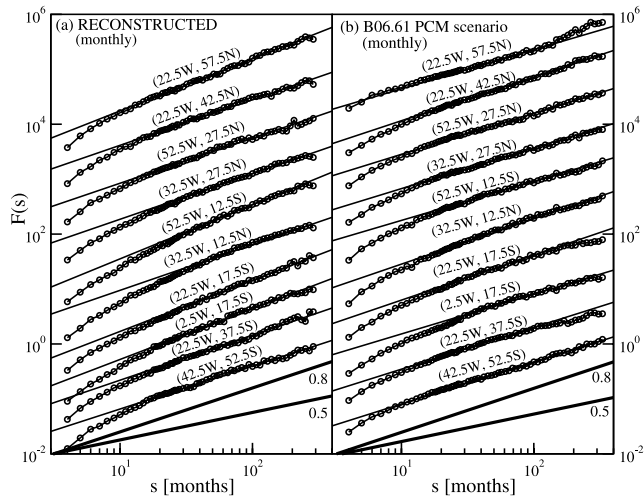


**Figure 2.** DFA2 fluctuation functions  $F(s)$  for monthly sea surface temperature anomalies at 10 sites in the Atlantic ocean: (a) the Kaplan reconstructed data and (b) NCAR PCM B06.61 (all forcings) run. The scale of  $F(s)$  is arbitrary. The straight lines crossing each curve represent the best asymptotic fit. The two lines shown at the bottom have slopes 0.8 and 0.5.

circulation dynamics. The variation of the scaling exponents over the Atlantic Ocean is significantly larger than on land, which is probably due to different ocean circulation patterns in equatorial, mid-latitude, and high-latitude regions. In a double logarithmic presentation, the slopes of the DFA2 curves for the simulated ocean records have an average of 0.72 which is noticeably lower than the observed average of 0.85.

[13] Figure 3 presents the fluctuation exponent distribution for the observed data and for the 10 NCAR PCM forced simulations considered for the 16 land locations. In each panel the “grey” column in the range [0.62, 0.68] represents the distribution of the fluctuation exponents for the observed data. As seen from the figure, forced simulations containing volcanic forcing best reproduce the observations since they have a peak at the same range [0.62, 0.68] as the observed data. Their average fluctuation exponent is close to 0.65. In contrast, the other six simulations that do not contain volcanic forcing, have an average fluctuation exponent for land less than 0.6 [see also *Govindan et al., 2002*].

[14] Similar behavior is found over the Atlantic Ocean. Only those simulations containing the volcanic forcing exhibit an average fluctuation exponent greater than 0.7 with the largest value equal to 0.76 for the volcanic forcing only simulation. Figure 4 shows the fluctuation exponent distribution for the Atlantic Ocean for the Kaplan data (in grey) and for 10 studied forced simulations (in black). Thus the PCM underestimates the fluctuation exponents obtained for Kaplan data for the Atlantic Ocean by 10–15%.

[15] Therefore, we can conclude that for the NCAR PCM addition of volcanic forcing to any other forcing combination immediately improves its scaling behavior both for the land and the ocean. This fact suggests that (besides the atmosphere-ocean coupling) the volcanic forcing is mostly responsible for the presence of the long-term correlations in the NCAR PCM over land on annual and decadal scales.

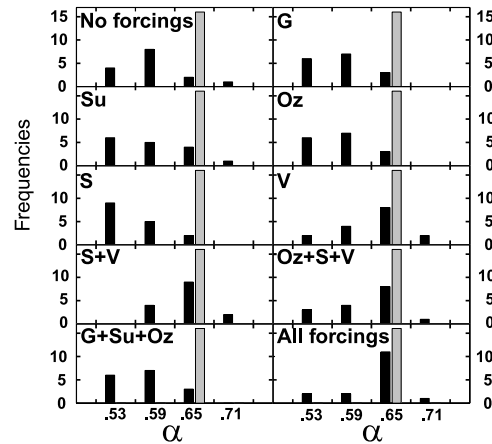


**Figure 3.** Histograms of the fluctuation exponents  $\alpha$  for the observed records (grey column) and the simulated records, for land stations. The considered 10 forcings are: no forcings, greenhouse gas (G), sulfate (Su), ozone (Oz), solar (S), volcanic (V), solar + volcanic (S + V), ozone + solar + volcanic (Oz + S + V), greenhouse gas + sulfate + ozone (G + Su + Oz), and all forcings. Four bins in each panel correspond to  $\alpha$  in the intervals [0.5, 0.56), [0.56, 0.62), [0.62, 0.68), and [0.68, 0.74] respectively. The bin size represents the error bar for the monthly DFA2 [*Peng et al., 1993*]. The grey column in each panel corresponds to the fluctuation exponent distribution for the observed records, the black columns are for simulated records.

For the ocean, the addition of volcanic forcing leads to stronger memory and consequently higher fluctuation exponents comparing to those for the land. However the NCAR PCM still underestimates the observed persistence of the oceans. It is possible that this deviation is due to the fact, that the modelled ocean is not filled with water and eddies but with a rather viscous fluid and laminar flow. The presence of small-scale noise affects the correlation function

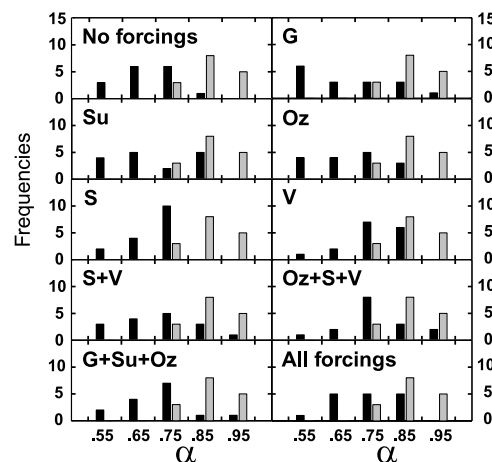


**Figure 4.** Histograms for the fluctuation exponents for the Kaplan reconstructed (in grey) and simulated (in black) records for the Atlantic Ocean. The five bins correspond to  $\alpha$  values in the intervals [0.5, 0.6), [0.6, 0.7), [0.7, 0.8), [0.8, 0.9), and [0.9, 1.0] respectively.

of large scale features [von Storch, 2004], and in ocean models such small scale noise is absent.

## 5. Conclusion

[16] The main conclusion from our research is that the NCAR PCM is able to reproduce the scaling behavior of the observed land SAT records for the last century after taking into account all historically based natural and anthropogenic forcings. However, even the best forced simulation for the land slightly underestimates natural SST persistence in the ocean, possibly due to errors in the simulations of deep ocean circulation, the atmosphere-ocean interaction, and/or an insufficiently long spin up period of the ocean component of the AOGCM.

[17] The results of the analysis of SAT fluctuation exponents for inner continental regions presented in this letter are in contrast with [Fraedrich and Blender, 2003]). Our study indicates that not only the observed records for inner continental regions are long-term correlated in agreement with [Bunde et al., 2004], but also the recent PCM simulations for these regions show similar fluctuation exponents, characteristic of long-term persistence.

[18] Finally, this letter also supports the suggestion of [Govindan et al., 2002] that the inability of the seven leading AOGCMs, for their control runs, greenhouse gas forcing only, and greenhouse gas plus aerosols forced simulations, to mimic the observed SAT persistence is caused by the absence of natural forcings, in particular volcanic forcing. The results of our detrended fluctuation analysis for the 16 land stations around the globe and the 16 sites in the Atlantic ocean suggest that volcanic forcing has by far the largest impact on the AOGCM long-memory persistence.

[19] **Acknowledgments.** This work has been supported by the Deutsche Forschungsgemeinschaft and the Israel Science Foundation. We are grateful to W. M. Washington, M. Wehner, and G. Strand for providing access to the NCAR PCM simulations data. The authors thank J. Eichner, J. Kantelhardt and E. Koscielny-Bunde for fruitful discussions.

## References

- Ammann, C. M., G. A. Meehl, W. M. Washington, and C. S. Zender (2003), A monthly and latitudinally varying volcanic forcing dataset in simulations of 20th century climate, *Geophys. Res. Lett.*, *30*(12), 1657, doi:10.1029/2003GL016875.
- Bell, J., P. Duffy, C. Covey, and L. Sloan (2000), Comparison of temperature variability in observations and sixteen climate model simulations, *Geophys. Res. Lett.*, *27*, 261–264.
- Blender, R., and K. Fraedrich (2003), Long Time Memory in Global Warming Simulations, *Geophys. Res. Lett.*, *30*(14), 1769, doi:10.1029/2003GL017666.
- Bunde, A., J. F. Eichner, S. Havlin, E. Koscielny-Bunde, H. J. Schellnhuber, and D. Vyushin (2004), Comment on “Scaling of atmosphere and ocean temperature correlations in observations and climate models”, *Phys. Rev. Lett.*, *92*, 039801.
- Caballero, R., S. Jewson, and A. Brix (2002), Long memory in surface air temperature: detection, modeling, and application to weather derivative valuation, *Clim. Res.*, *21*(2), 127.
- Dai, A., T. M. L. Wigley, B. A. Boville, J. T. Kiehl, and L. E. Buja (2001), Climates of the twentieth and twenty-first centuries simulated by the NCAR climate system model, *J. Clim.*, *14*, 485–519.
- Eichner, J. F., E. Koscielny-Bunde, A. Bunde, S. Havlin, and H. J. Schellnhuber (2003), Power-law persistence and trends in the atmosphere: a detailed study of long temperature records, *Phys. Rev. E*, *68*, 046133.
- Fraedrich, K., and R. Blender (2003), Scaling of Atmosphere and Ocean Temperature Correlations on Observations and Climate Models, *Phys. Rev. Lett.*, *90*, 108501.
- Govindan, R. B., D. Vyushin, S. Brenner, A. Bunde, S. Havlin, and H. J. Schellnhuber (2001), Long-range correlations and trends in global climate models: Comparison with real data, *Physica A*, *294*, 239.
- Govindan, R. B., D. Vyushin, A. Bunde, S. Brenner, S. Havlin, and H. J. Schellnhuber (2002), Global climate models violate scaling of the observed atmospheric variability, *Phys. Rev. Lett.*, *89*, 028501.
- Hoyt, D. V., and K. H. Schatten (1993), A discussion of plausible solar irradiance variations, 1700–1992, *J. Geophys. Res.*, *98*(A11), 18,895–18,906.
- Kantelhardt, J. W., E. Koscielny-Bunde, H. H. A. Rego, S. Havlin, and A. Bunde (2001), Detecting long-range correlations with detrended fluctuation analysis, *Physica A*, *295*, 441.
- Kaplan, A., M. A. Cane, Y. Kushnir, A. C. Clement, M. B. Blumenthal, and B. Rajagopalan (1998), Analyses of global sea surface temperature 1856–1991, *J. Geophys. Res.*, *103*(C9), 18,567–18,589.
- Kiehl, J. T., T. L. Schneider, P. J. Rasch, M. C. Barth, and J. Wong (2000), Radiative forcing due to sulfate aerosols from simulations with the National Center for Atmospheric Research Community Climate Model, Version 3, *J. Geophys. Res.*, *105*(D1), 1441–1458.
- Koscielny-Bunde, E., A. Bunde, S. Havlin, and Y. Goldreich (1996), Analysis of daily temperature fluctuations, *Physica A*, *231*, 393.
- Koscielny-Bunde, E., A. Bunde, S. Havlin, H. E. Roman, Y. Goldreich, and H. J. Schellnhuber (1998), Indication of a universal persistence law governing atmospheric variability, *Phys. Rev. Lett.*, *81*, 729–732.
- Manabe, S., and R. Stouffer (1996), Low-Frequency Variability of Surface Air Temperature in a 1000-Year Integration of a Coupled Atmosphere-Ocean-Land Surface Model, *J. Clim.*, *9*, 376–393.
- Meehl, G. A., W. M. Washington, T. M. L. Wigley, J. M. Arblaster, and A. Dai (2003), Solar and greenhouse gas forcing and climate response in the twentieth century, *J. Clim.*, *16*, 426–444.
- Mitchell, J. F. B., et al. (2001), Detection of Climate change and Attribution of Causes, in *Climate Change 2001: The Scientific Basis, Contribution of Working Group I to the Third Assessment, Report of the IPCC*, edited by J. T. Houghton et al., pp. 695–738, Cambridge Univ. Press, New York.
- Monetti, R. A., S. Havlin, and A. Bunde (2003), Long term persistence in the sea surface temperature fluctuations, *Physica A*, *320*, 581–590.
- Parker, D. E., P. D. Jones, C. K. Folland, and A. Bevan (1994), Interdecadal changes of surface temperature since the late nineteenth century, *J. Geophys. Res.*, *99*(D7), 14,373–14,400.
- Pelletier, J. D., and D. L. Turcotte (1997), Long-range persistence in climatological and hydrological time series: analysis, modeling and application to drought hazard assessment, *J. Hydrol.*, *203*, 198–208.
- Pelletier, J. D. (2002), Natural variability of atmospheric temperatures and geomagnetic intensity over a wide range of time scales, *Proc. Natl. Acad. Sci. U. S. A.*, *99*, 2546–2553.
- Peng, C.-K., S. V. Buldyrev, A. L. Goldberger, S. Havlin, M. Simons, and H. E. Stanley (1993), Finite-size effects on long-range correlations: Implications for analyzing DNA sequences, *Phys. Rev. E*, *47*(5), 3730–3733.
- Peng, C.-K., S. V. Buldyrev, S. Havlin, M. Simons, H. E. Stanley, and A. L. Goldberger (1994), On the mosaic organization of DNA nucleotides, *Phys. Rev. E*, *49*(2), 1685–1689.
- Reynolds, R., and T. Smith (1994), Improved global sea-surface temperature analyses using optimum interpolation, *J. Clim.*, *7*, 929–948.
- von Storch, H., and G. Floeser (Eds.) (1999), *Anthropogenic Climate Change*, Springer Verlag; Berlin, Heidelberg.
- von Storch, J.-S. (2004), On statistical dissipation in GCM-climate, *Clim. Dyn.*, (in press).
- Syrocka, J., and R. Toumi (2001), Scaling and persistence in observed and modelled surface temperature, *Geophys. Res. Lett.*, *28*(17), 3255–3258.
- Talkner, P., and R. O. Weber (2000), Power spectrum and detrended fluctuation analysis: Application to daily temperatures, *Phys. Rev. E*, *62*, 150.
- Vyushin, D., R. B. Govindan, S. Brenner, A. Bunde, S. Havlin, and H. J. Schellnhuber (2002), Lack of scaling in global climate models, *J. Phys. Condens. Matter*, *14*, 2275–2285.
- Washington, W. M., et al. (2000), Parallel Climate Model (PCM) control and transient simulations, *Clim. Dyn.*, *16*, 755–774.

S. Brenner, Department of Geography, Bar-Ilan University, Ramat-Gan 52900, Israel. (sbrenner@mail.biu.ac.il)

A. Bunde, Institut für Theoretische Physik III, Justus-Liebig-Universität Giessen, Heinrich-Buff-Ring 16, 35392 Giessen, Germany. (armin.bunde@theo.physik.uni-giessen.de)

S. Havlin, D. Vyushin, and I. Zhidkov, Minerva Center and Department of Physics, Bar-Ilan University, Ramat-Gan 52900, Israel. (havlin@ophir.ph.biu.ac.il; vyushin@ory.ph.biu.ac.il; zhidkov@shoshi.ph.biu.ac.il)